Published in final edited form as:
Free Radic Biol Med. 2012 July 1; 53(1): 172–181. doi:10.1016/j.freeradbiomed.2012.04.023.

Free radical-operated proteotoxic stress in macrophages primed with lipopolysaccharide

Dili Zhai[a,1], **Sandra E. Gomez-Mejiba**[b,1], **Maria S. Gimenez**[b], **Leesa J. Deter ding**[c,2], **Kenneth B. Tomer**[c,2], **Ronald P. Mason**[d,2], **Michael T. Ashby**[e], and **Dario C. Ramirez**[b,f,*]

[a]Department of Medicine, Gastroenterology Section, University of Chicago, Chicago, IL 60637, USA

[b]Laboratory of Experimental and Therapeutic Medicine, Instituto Multidisciplinario de Investigaciones Biológicas-San Luis (IMIBIO-SL)-Consejo Nacional de Investigaciones Científicas y Tecnológicas (CONICET), San Luis, San Luis 5700, Argentina

[c]Laboratory of Structural Biology, NIEHS, National Institutes of Health, Research Triangle Park, NC 27709, USA

[d]Laboratory of Pharmacology and Chemistry, NIEHS, National Institutes of Health, Research Triangle Park, NC 27709, USA

[e]Department of Chemistry and Biochemistry, University of Oklahoma, Norman, OK 73019, USA

[f]Department of Biochemistry and Biological Sciences, School of Chemistry, Biochemistry and Pharmacy, National University of San Luis, San Luis, San Luis 5700, Argentina

Abstract

The free-radical-operated mechanism of death of activated macrophages at sites of inflammation is unclear, but it is important to define it in order to find targets to prevent further tissue dysfunction. A well-defined model of macrophage activation at sites of inflammation is the treatment of RAW 264.7 cells with lipopolysaccharide (LPS), with the resulting production of reactive oxygen species (ROS). ROS and other free radicals can be trapped with the nitrone spin trap 5,5-dimethyl-1-pyrroline *N*-oxide (DMPO), a cell-permeable probe with antioxidant properties, which thus interferes with free-radical-operated oxidation processes. Here we have used immuno-spin trapping to investigate the role of free-radical-operated protein oxidation in LPS-induced cytotoxicity in macrophages. Treatment of RAW 264.7 cells with LPS resulted in increased ROS production, oxidation of proteins, cell morphological changes and cytotoxicity. DMPO was found to trap protein radicals to form protein–DMPO nitrone adducts, to reduce protein carbonyls, and to block LPS-induced cell death. *N*-Acetylcysteine (a source of reduced glutathione), diphenyleneiodonium (an inhibitor of NADPH oxidase), and 2,2′-dipyridyl (a chelator of Fe^{2+}) prevented LPS-induced oxidative stress and cell death and reduced DMPO–

*Corresponding author at: Laboratory of Experimental and Therapeutic Medicine, IMIBIO-SL-CONICET and Molecular Genetics, Universidad Nacional de San Luis, Av. Ejercito de los Andes 950, San Luis, 5700 San Luis, Argentina. ramirezlabimibiosl@ymail.com (D.C. Ramirez).

[1]Contributed equally to this work.

[2]Part of the Intramural Research Program of the NIEHS, NIH.

nitrone adduct formation, suggesting a critical role of ROS, metals, and protein-radical formation in LPS-induced cell cytotoxicity. We also determined the subcellular localization of protein–DMPO nitrone adducts and identified some candidate proteins for DMPO attachment by LC-MS/MS. The LC-MS/MS data are consistent with glyceraldehyde-3-phosphate dehydrogenase, one of the most abundant, sensitive, and ubiquitous proteins in the cell, becoming labeled with DMPO when the cell is primed with LPS. This information will help find strategies to treat inflammation-associated tissue dysfunction by focusing on preventing free radical-operated proteotoxic stress and death of macrophages.

Keywords

Macrophage; Lipopolysaccharide; Reactive oxygen species; Protein oxidation; Spin trapping; Antioxidant

Introduction

Inflammatory activation of macrophages occurs in atheromatous plaques [1], inflamed adipose tissue in obesity [2,3], and tumors [4]. This activation is associated with the death of macrophages and tissue dysfunction [5], but the role of free-radical-operated processes has not received the attention it deserves—mostly due to the limitations of studying them in biological systems. Treatment of macrophages with bacterial lipopolysaccharide (LPS) is a well-established model for studying the fate of macrophages at sites of inflammation [6].

A number of reactive oxygen species (ROS) are produced inside macrophages primed with LPS. For instance, superoxide radical anion ($^{\bullet}O_2^-$) is produced primarily, but not exclusively, by NADPH oxidases [7–9]. Other recognized sources of $^{\bullet}O_2^-$ in activated macrophages are mitochondria [10], uncoupling of inducible nitric oxide synthase (iNOS) [11], and endoplasmic reticulum stress [12,13]. Another reactive species, nitric oxide ($^{\bullet}NO$), is produced by iNOS in RAW 264.7 cells and primary macrophages primed with LPS [14]. Superoxide can be dismutated to hydrogen peroxide (H_2O_2) by superoxide dismutase, or it can react with $^{\bullet}NO$ to form peroxynitrite [15,16]. Peroxynitrite has been shown to nitrate proteins in cells with the intermediacy of transient protein-centered radicals [17].

H_2O_2, a cell-permeable, two-electron oxidant, cannot cause protein-centered radicals due to its low chemical reactivity; however, H_2O_2 reactivity can be enhanced by redox-active transition metals, either free or bound to proteins, to produce hydroxyl radicals [18,19]. Hydroxyl radicals can randomly damage lipids, proteins, and nucleic acids with the formation of macromolecule-centered free radicals as transient intermediates [20,21]. Decay of these intermediates is a complex process that depends on a number of microenvironmental cues [22,23]; one of the most characterized mechanisms is their reaction with molecular dioxygen to form peroxyl radicals [22]. Peroxyl radicals decompose to produce a number of end-oxidation products.

In the case of protein-centered radicals, the end products include aldehydes and carbonyls [22]. Although carbonyl formation in proteins is considered a marker of protein oxidation by

free radical processes [18], a number of reactive lipid oxidation-derived carbonyl products (e.g., 4-hydroxynonenal) can form adducts with proteins, resulting in increased protein carbonylation [24,25]. This class of reactions compromises the specificity of carbonyls as markers of free radical-mediated protein oxidation processes. Therefore, the detection of protein-centered radicals is a critical proof of protein oxidation by one-electron or free-radical-operated oxidation mechanisms.

Characterization of protein-centered radicals in biochemistry has been possible since the development of electron spin resonance (ESR), the conventional technique that is used to study free radicals [26]. However, because free radicals are unstable and highly reactive species, their detection in cells was a challenge until the development of spin trapping [27]. Spin trapping makes use of organic compounds to react with the free radicals to produce radical adducts with longer half-lives and thus facilitate their detection by ESR [28]. 5,5-Dimethy-l-pyrroline *N*-oxide (DMPO), a nitrone spin trap, passes across cell membranes, effectively traps a number of small and large free radicals, and possesses low toxicity [27], making it a good spin trap for investigating free radicals in biological systems.

We have previously found that protein-centered radicals that are trapped by DMPO as nitrone adducts are protected from further oxidation [21]. Herein, we hypothesized that if free radical operated processes are involved in LPS-induced cell damage, then DMPO should be able to affect this process and at the same time “tag” specific macromolecules undergoing one-electron oxidation, which might or might not be directly involved in the death process. To test our hypothesis, we have here used the DMPO-based immuno-spin trapping technique ([29] and references therein). This technique is based on the use of DMPO, which traps protein-, lipid-, carbohydrate-, and nucleic acid-centered radicals to form radical adducts which then decay to stable nitrone adducts. Protein- and DNA-nitrone adducts can be subsequently determined by immunoassays using an anti-DMPO serum and mass spectrometry methods [30,31].

We found that DMPO prevented LPS-induced proteotoxic damage in macrophages and tagged a number of proteins inside the cell. We corroborated the identity of glyceraldehyde-3-phosphate dehydrogenase (GAPDH, EC 1.2.1.12), one of the most ubiquitous, abundant, and redox-sensitive proteins in cells [32], as one of the major targets of free radical-mediated oxidation in cells primed with LPS. The information gathered herein will help in understanding how free radical-operated protein oxidation occurs during macrophage death at sites of inflammation, and thus will provide new avenues for intervention in subsequent tissue dysfunction processes.

Materials and methods

Materials

Murine macrophage-like RAW 264.7 cells were purchased from the American Type Culture Collection (TIB-71, Rockville, MD). DMPO (ε_{228} = 7800 M^{-1} cm^{-1}) and rabbit polyclonal anti-DMPO antibody were purchased from Alexis Biochemicals (San Diego, CA). LPS (*Escherichia coli* serotype 055:B5, L2637), *N*-acetylcysteine (NAC), and rabbit anti-dinitrophenyl were from Sigma (St. Louis, MO). The goat anti-rabbit IgG and goat anti-

mouse IgG conjugated with horseradish peroxidase (HRP) were from Santa Cruz Biotechnology (Santa Cruz, CA).

Cell culture and treatments with LPS and DMPO

RAW 264.7 cells were cultured in high-glucose Dulbecco's modified Eagle's medium (Sigma, D-5796) supplemented with 10% fetal bovine serum (Advantage FBS, Atlanta Biologicals, Lawrenceville, GA), referred to as complete medium. Cells were maintained in a humidified atmosphere of 5% CO_2 at 37°C and split 2–3 times weekly. Cells between passages 3 and 30 were used in this study. Before the treatments with LPS and DMPO, cells were allowed to stabilize overnight. Medium was then removed and replaced by the indicated concentrations of LPS and/or DMPO in complete medium. Typically, cells were incubated for 24 h in complete medium containing 1 ng/ml LPS and 50 mM DMPO.

Cytotoxicity assays

Cell viability was determined by assaying mitochondrial reduction of a yellow tetrazolium salt, 3-(4,5-dimethylthiazol-2-yl)-2,5-diphenyltetrazolium bromide (MTT), to purple formazan crystals [33]. We also assessed the release of lactate dehydrogenase (LDH) to the culture medium as a marker of membrane damage by using a commercial kit (Bioassay Systems, Hayward, CA). Alternatively, we measured cell viability by assessing total cell protein and DNA remaining bound to culture plates after the described treatments and three washes with PBS to remove unattached (nonviable) macrophages. Briefly, cells were grown and treated with LPS and DMPO in black-walled, clear-bottom, 96-well plates (BD Biosciences, San Jose, CA), and DNA was quantified using a CyQUANT cell proliferation assay kit (Invitrogen) and bacteriophage λ DNA as a standard. In another experiment, after a rinse of the monolayers with PBS, proteins bound to the plate were dissolved in 50 μl of 1 M NaOH followed by determination of proteins using a BCA (bicinchoninic acid) protein assay kit (Thermo Fisher Scientific, Rockford, IL).

Measurement of ROS production

Intracellular ROS production was estimated using carboxy-H_2DCFDA, which becomes fluorescent in living cells in response to various ROS including ●OH, H_2O_2, and $ONOO^-$ [34]. Cells were incubated with 25 μM carboxy-H_2DCFDA for 30 min, washed twice, and then treated with 0 to 1 ng/ml LPS for another 30 min. ROS production was quantified based on the fluorescence intensity at excitation/emission λ = 495/529 nm using an Infinite M200 plate reader (Tecan, Research Triangle Park, NC).

Assessment of morphological changes

Cells were grown on 8-well LabTek culture glass slides (Nalge Nunc International, Rochester, NY). After treatment with 0, 0.25, 0.50, or 1 ng/ml LPS and/or 50 mM DMPO for 24 h, cells were washed with PBS, fixed, and then stained using a Diff-Quick stain kit (IMEB Inc., San Marcos, CA) and mounted with Permount (Thermo Fisher Scientific). The cell morphology of stained cells was observed and acquired using an inverted light microscope at 400x magnification. Additionally, images of living cells were taken directly

under an inverted phase-contrast digital microscope (Jenco International, Inc., Portland, OR).

Preparation of cell homogenates

Cells were grown in T75 culture flasks (Cellstar, Greiner Bio-One, Frickenhausen, Germany) in the absence and presence of 0.25, 0.5, and 1 ng/ml LPS and/or 50 mM DMPO. After 24 h incubation, cells were gently scraped off and washed with ice-cold PBS, pH 7.4. Cells were homogenized in ice-cold lysis buffer (50 mM Tris–HCl, pH 8.0, 1% Nonidet P-40, 0.25% sodium deoxycholate, 1 mM diethylenetriaminepentaacetic acid, 1 mM Na_3VO_4, 1 mM NaF, and 150 mM NaCl) containing 1% (v/v) protease inhibitor cocktail (Amresco, Solon, OH) and 25 U/ml of Benzonase nuclease (Novagen, Madison, WI). The supernatant was collected by centrifugation (11,700 g for 15 min at 4°C), and total protein was determined using a BCA protein assay kit.

Cell fractionation

RAW 264.7 cells were incubated for 24 h in complete medium with 1 ng/ml LPS and 50 mM DMPO. After treatment, cells were harvested and subcellular fractions were prepared as described by Bronfman et al. [35]. Briefly, after rinsing and harvesting with PBS, cells were resuspended in an ice-cold buffer (0.25 M sucrose and 3 mM imidazole, pH 7.4) containing 0.1% digitonin to permeabilize the cells. Cells were broken by 10 passages through a Dounce homogenizer while on ice. Broken cells were centrifuged and the pellet (nuclear) fraction was separated from the cytoplasm. After a sequence of subsequent centrifugations, the cytoplasmic fraction was separated into mitochondrial, lysosomal, microsomal, and cytosolic fractions. The protein concentration in each fraction was adjusted and analyzed for specific markers [35] by Western blot. Nitrone adducts in each fraction were analyzed by enzyme-linked immunosorbent assay (ELISA). See below.

Determination of protein carbonyls

Protein carbonyls were determined in cell homogenates using an ELISA [36] with some modifications. Briefly, cell homogenates were derivatized to 2,4-dinitrophenylhydrazone by reaction with 2,4-dinitrophenylhydrazine in 2 M HCl. Ten microliters of the derivatized or nonderivatized sample were added to 190 μl of 0.1 M bicarbonate buffer, pH 9.6, in white 96-well ELISA plates (Corning Incorporated, Corning, NY) and incubated overnight at 4°C. Following washing with 0.05% Tween 20 in PBS and blocking with 2.5% cold-water fish skin gelatin (Sigma) in PBS at 37°C for 1 h, the plates were incubated for 1 h at 37°C with the rabbit polyclonal anti-dinitrophenyl (1:1,000 dilution) antibody. The immunocomplexes were quantified using goat anti-rabbit IgG-HRP conjugate and VisiGlo Chemilu HRP substrate solution (Amresco) and the luminescence was read using a microplate reader.

Measurement of protein-DMPO nitrone adducts in cell homogenates and subcellular fractions

The nitrone adducts in whole homogenate or subcellular fractions from cells treated with or without LPS and/or DMPO were determined by ELISA [37].

Determination of total nitrone adducts in cells

We used a cell-based ELISA and immunocytochemistry to quantify and localize protein-DMPO nitrone adducts in LPS-activated cells. Cells were incubated in transparent, flat-bottom, 96-well microplates. After treatment with LPS and/or DMPO, cells were fixed with 4% paraformaldehyde (Electron Microscopy Sciences, Hatfield, PA) in PBS for 15 min, followed by −20°C-methanol permeabilization for 2 min and treatment with 10 mM sodium cyanide for 15 min to inhibit endogenous peroxidases. After blocking with 1% fat-free milk at 37°C for 1 h, cells were incubated with a 1:5000 dilution of rabbit polyclonal anti-DMPO in washing buffer at 37 C for 1 h. Cells were washed 3 times with washing buffer and incubated with goat anti-rabbit IgG conjugated with HRP (1:5000) for 1 h at 37°C. Peroxidase activity was developed with 50 μl of a 1-Step Ultra TMB-ELISA kit (Thermo Fisher Scientific) and the reaction stopped by addition of an equal volume of 2 M sulfuric acid. Absorbance at 450 nm was recorded using a microplate reader and adjusted by a parallel protein assay to normalize the cell number among the treatment groups. Note that the anti-DMPO serum recognizes DMPO but not the molecule to which DMPO is bound [30]. In this case, the interference by free DMPO and small molecule-DMPO nitrone adducts was effectively ruled out by a series of fixation, permeabilization, and extensive washing steps before exposure of the cells to the anti-DMPO serum.

Western blot analysis of nitrone adducts

Cell homogenates (2.5 mg/ml) were mixed with 4X SDS NuPAGE sample loading buffer (Invitrogen) and 100 mM 2-mercaptoethanol. After heat denaturation, equal amounts of cellular protein (15 μg/lane) were separated on 4–12% reducing NuPAGE Bis-Tris Gels (Invitrogen), followed by blotting onto a nitrocellulose membrane using a semidry transfer apparatus (BioRad Laboratories, Hercules, CA). After blocking with 1% nonfat milk in PBS, the immunoblot was performed by incubation with a primary antibody in washing buffer (0.1% milk in PBS/0.05% Tween 20) overnight at 4°C, followed by incubation with an HRP-conjugated secondary antibody (1:1000 dilution) for 1 h at room temperature. The immunocomplexes were visualized using SuperSignal West Pico Chemiluminescent HRP Substrate (Thermo Fisher Scientific) and recorded by a FluorChem HD2 Imager (Alpha Innotech Corp., San Leandro, CA). For primary antibodies, rabbit polyclonal antiserum against DMPO (1:1000 dilution) and mouse monoclonal antibody against β-actin (1:2500 dilution) were used.

Immunocytochemistry of nitrone adducts in cells

Cells were grown on cover glasses (22 mm × 22 mm, Thermo Fisher Scientific). To localize nitrone adducts after the treatments, cells were fixed with 4% paraformaldehyde for 15 min at room temperature. Cells were blocked with 2% bovine serum albumin at room temperature for 1 h. After that, cells were serially incubated with rabbit anti-DMPO (1:500 dilution) and goat anti-rabbit Alexa Fluor 488 at 37°C for 1 h. Finally, cells were rinsed in PBS, mounted on cover glasses with Prolong Gold antifade reagent with 4′-6-diamidino-2-phenylindole (DAPI, Invitrogen), and the immunostaining was examined by confocal imaging using a Leica SP2 MP confocal microscope with a 63 × 1.4 oil immersion objective. A sequence of 23 single-planar images was acquired to show intracellular

localization of nitrone adducts. In these images, the analysis of the green fluorescence intensity due to nitrone adducts was performed, on an image in which the DAPI signal blue channel was turned off, on a PC computer using the public domain NIH Image J program (developed at the U.S. National Institutes of Health and available on the Internet at http://rsb.info.nih.gov/nih-image/).

Immunoprecipitation

We prepared an anti-DMPO and anti-GAPDH molecular "catcher" by incubating a monoclonal antibody anti-DMPO or anti-GAPDH with a goat anti-mouse IgG magnetic bead, followed by covalent cross-linking with 1-ethyl-3-[3-dimethyl-aminopropyl] carbodiimide hydrochloride (EDC, Thermo Fisher Scientific) as suggested by the manufacturer. As a control, we used a similar procedure to conjugate a monoclonal antibody, anti-mouse β-actin. Macrophage homogenates were adjusted to 2.5 mg/ml in PBS containing 0.5% Tween 20 (washing buffer) to minimize nonspecific binding of proteins to the catchers and incubated overnight at 4°C. After incubation, the immunocomplexes (see Fig. 4C) were isolated with a magnet, washed three times with washing buffer, and resuspended in 50 μl of elution buffer (Thermo Fisher Scientific). After removal of the beads with the magnetic field, the solution of eluted proteins was mixed with 10 μl of sample buffer and 5 μl of 2-mercaptoethanol and separated on 4–12% reducing NuPAGE Bis-Tris Gels. Gels were stained with Coomassie blue to identify proteins by MS analysis or blotted onto a nitrocellulose membrane and Western-blotted using rabbit anti-DMPO.

Mass spectrometric analysis

The bands of proteins identified to be positive in the anti-DMPO Western blot were excised from a one-dimensional gel rather than a two-dimensional gel because the thiourea treatment during sample preparation for two-dimensional electrophoresis produced the release of DMPO from the protein–DMPO nitrone adduct (data not shown). For instance, we reported that the treatment of preformed hemoglobin nitrone adducts with 1 M 2-mercaptoethanol or thiourea for 10 min with or without heating of the sample produced a loss of DMPO immunoreactivity [37]. This observation remains to be explained, but is most likely due to the nucleophilic displacement of DMPO from the protein by the thiol compound. Liquid chromatography (LC)–MS/MS analysis and data analysis were performed following the same method described previously [38].

Statistical analysis

The quantitative data are reported as the mean values ± standard error of the mean (SEM). We determined the significance of differences between pairs by Student's *t* test and between treatments and control by one-way ANOVA with Dunnett's post hoc testing. $P < 0.05$ was considered as statistically significant.

Results

LPS induces ROS and cytotoxicity in RAW 264.7 cells

To determine the lowest concentration of LPS needed to induce cytotoxicity, we incubated RAW 264.7 cells with increasing concentrations of LPS ranging from 0 to 100 ng/ml for 24

h (Fig. 1A). A significant loss (approximately 30%) of cell viability occurred when the cells were treated for 24 h with 1 ng/ml LPS (Fig. 1A). Interestingly, a further loss of less than 10% viability (total loss of viability about 40%) was observed when cells were exposed to LPS from 1 to 100 ng/ml. A pattern similar to that observed in Fig. 1A was obtained by measuring LDH released to the medium or protein and DNA bound to the bottom of the culture plate (data not shown). As shown in Fig. 1B, low concentrations of LPS were able to induce DCFH oxidation in macrophages as measured using the fluorescent probe carboxy-H_2DCFDA. Moreover, cells treated with increasing concentrations of LPS for 24 h underwent dramatic morphological changes characterized by hypertrophy and extensive vacuolization (Fig. 1C, arrowhead). This LPS-induced cell vacuolization was accompanied by loss of cell viability as shown in Fig. 1A. In addition, approximately 60% of cells increased 2− to 4-fold in size after 24 h treatment with LPS of 1 ng/ml or higher.

DMPO prevents protein carbonyl accumulation and cytotoxicity induced by LPS in RAW 264.7 cells

We then hypothesized that DMPO can prevent cytotoxicity induced by LPS by blocking free-radical-dependent processes that lead to accumulation of end-oxidation products, such as carbonylated proteins. To trap free radicals inside the cell, high concentrations of DMPO are required to efficiently compete with fast free-radical decay mechanisms, such as radical–radical reactions, production of oxidation end-products, and scavenging by antioxidants [29]. However, high doses of DMPO can also produce cytotoxicity. When 3.1–50 mM DMPO was present in the culture medium for 24 h, DMPO caused no significant cytotoxicity as assessed by mitochondrial function (MTT reduction to formazan) and cellular DNA or proteins in cells attached to the culture plate (Fig. 2A). Interestingly, DMPO protected cells against LPS-induced cytotoxicity (Fig. 2B). Determination of the release of LDH and trypan blue exclusion, two markers of membrane-selectivity integrity, showed similar results (data not shown). To completely protect against LPS-induced RAW 264.7 cell damage, it was necessary to add DMPO no later than 1 h after LPS stimulation (Fig. 2C). Indeed, when DMPO was added at more than 6 h after LPS addition, it produced no cytoprotective effects (Fig. 2C). DMPO (50 mM) also inhibited LPS-induced cell morphological changes (Fig. 2D), presumably as a consequence of trapping of free radicals. The inhibitory effect of DMPO shown in Fig. 2D was concentration-dependent (data not shown).

By trapping free radicals, DMPO might protect RAW 264.7 cells against LPS-induced accumulation of protein-carbonyls and other macromolecule-derived end-oxidation products. DMPO binds to proteins undergoing free-radical-operated oxidation to form nitrone adducts, and carbonyl formation is circumvented. A number of ROS formed in LPS-primed macrophages can oxidize proteins with formation of transient protein radicals as intermediates. Interestingly, similar effects were observed when macrophages were pretreated with either 2,2′-dipyridyl (DP), a ferrous iron chelator; diphenyleneiodonium (DPI), a NADPH oxidase inhibitor; or *N*-acetylcysteine (NAC), a source of intracellular decreased glutathione (Fig. 2E). DP, DPI, and NAC reduced LPS-induced changes in cell viability, protein carbonyls, and nitrone adduct formation, whereas DMSO did not affect these parameters.

DMPO traps protein-centered radicals in specific cell compartments

Interestingly, DMPO blocked LPS-induced protein carbonyls and known (direct and indirect) end-oxidation products of proteins in a concentration-dependent manner [18,25] (Fig. 3A). Based on these results we hypothesized that DMPO inhibits LPS-induced cell damage, at least in part, due to trapping of protein radicals, thereby preventing accumulation of carbonyls. To test this hypothesis, we analyzed protein-centered radicals using DMPO-based immuno-spin trapping assays [29]. We measured protein-DMPO nitrone adducts with a novel cell-based ELISA assay (Fig. 3B). Formation of intracellular protein-DMPO nitrone adducts was dependent on both LPS (0–1000 ng/ml) and DMPO (0–50 mM) concentrations (Fig. 3B).

To define the subcellular distribution of DMPO–nitrone adducts, we localized them by confocal microscopy using the anti-DMPO antibody. Fig. 3C shows the typical distribution of nitrone adducts inside cells treated with LPS and DMPO. The inset shows an image of a high-power magnification of a single and representative cell to highlight the perinuclear distribution of the nitrone adducts (arrowhead in Fig. 3C). To corroborate this pattern of distribution of nitrone adducts, we obtained a stack of 23 planar images in a representative cell. Fig. 3D shows the variation in the nitrone-adduct fluorescence intensity in each one of these 23 optical planes. Overall, Figs. 3C and 3D suggest that most of the nitrone adducts are localized in the perinuclear region of the cell. To verify these data, we performed the subcellular fractionation of cells treated with LPS and DMPO in cytosolic, nuclear, mitochondrial, lysosomal, and microsomal fractions. Nitrone adducts were quantified by ELISA in each one of these fractions (Fig. 3E). Interestingly, most of the nitrone adducts were found in the microsomal (~40%) and mitochondrial (~25%) fractions with respect to the whole cell homogenate (100%).

Identification of proteins tagged with DMPO in RAW 264.7 cells primed with LPS

To identify proteins tagged with DMPO, we analyzed total homogenates of macrophages treated with LPS and DMPO using an anti-DMPO Western blot and tandem-MS. Western blot analysis of these homogenates showed at least 16 bands that reacted with the anti-DMPO antibody (Fig. 4A). The formation of protein–DMPO nitrone adducts was DMPO concentration-dependent as confirmed by Western blot of the whole homogenates of cells incubated with 1 ng/ml LPS and varying concentrations of DMPO (0–50 mM) (see also Fig. 3B). Although two-dimensional electrophoresis would facilitate the identification of these DMPO-labeled proteins, our immuno-spin trapping assay is incompatible with this separation for reasons described in Materials and Methods (see Supplementary Fig. 1). The positive bands in the anti-DMPO Western blot analysis were localized in a Coomassie blue-stained gel run in parallel (Fig. 4B). The excised protein bands of interest were digested, and candidate proteins that potentially form nitrone adducts were identified by LC-MS/MS analysis (Supplementary Table 1).

In three separate experiments, we identified similar proteins in 7 of the 16 bands that were positive in our anti-DMPO Western blot (Fig. 4B). The proteins identified in the other 9 bands were also similar, but in our anti-DMPO Western blot, their intensity and/or intensity variation with the concentration of LPS or DMPO was less evident (see Fig. 4A). In

addition, most of the candidate proteins identified in the above 7 bands (Supplementary Table 1) could be categorized into several families involving signaling, endoplasmic reticulum stress (e.g., protein disulfide isomerase and a number of other chaperones), mitochondrial (e.g., aconitase), glycolytic metabolism (e.g., carbonic anhydrase, enolase, and GAPDH), and the cytoskeleton (e.g., actin and tubulin).

Importantly, proteins identified in these bands might or might not be proteins labeled with DMPO. For instance, we rationalized that some proteins not labeled with DMPO can be physically associated with proteins that are labeled with the spin trap. These proteins may be pulled down as a complex in our immunoprecipitations. Therefore, we verified the identity of one of those proteins forming adducts with DMPO: We used an anti-DMPO molecular "catcher" (Fig. 4C) to immunoprecipitate nitrone adducts from a homogenate of macrophages treated with 1 ng/ml of LPS and 50 mM of DMPO for 24 h, followed by one-dimensional electrophoresis analysis (Fig. 4D). This analysis showed several proteins, among them a band around 37 kDa (Fig. 4D). This band corresponds to band number six in the anti-DMPO Western blot and Coomassie blue staining shown in Figs. 4A and 4B, respectively (see also Supplementary Table 1). MS data are consistent with GAPDH in this band, and an anti-DMPO Western blot analysis of an immunoprecipitated protein of approximately 37 kDa molecular weight confirmed a nitrone adduct (Fig. 4D, lower panel). Furthermore, immunoprecipitation of GAPDH from cells treated with 50 mM DMPO showed an LPS-dependent formation of a GAPDH-DMPO nitrone adduct (Fig. 4E).

Discussion

Our findings show that protein-centered radicals are produced during ROS-dependent proteotoxic stress caused by low doses of LPS in RAW 264.7 cells. The cell-permeable nitrone spin trap DMPO binds to free radical sites in macromolecules undergoing oxidation [29,39], thereby preventing accumulation of toxic end-oxidation products and cytotoxicity. In addition, because of this property of DMPO to "tag" radical sites, it is possible to determine the subcellular distribution and identify proteins that are undergoing free radical-operating oxidation in stressed cells.

Exaggerated production of ROS, deregulation of metal compartmentalization, expression of peroxidases, and accumulation of oxidized proteins are important sources of stress in macrophages at sites of inflammation [22,23]. Antioxidants such as L-ascorbate and reduced glutathione scavenge free radicals, sometimes becoming radicals themselves [40]. For instance, L-ascorbate reacts with radical sites in proteins at rates between 10^7 and 10^8 M^{-1} s^{-1}, depending on the location of the radical in the protein, to form an ascorbyl radical and repair the protein [41]. Spin traps are also antioxidants, but they bind covalently to free radical sites in macromolecules [20,26]. Although spin traps were originally developed to increase the half-life of free radicals to facilitate their study by ESR [28], recent evidence indicates that they might be useful as anti-inflammatory drugs [42,43]. The rationale behind this therapeutic application of spin traps is that oxidized macromolecules can cause proteotoxic stress in cells; thus, prevention of accumulation of oxidized products and death of macrophages with a spin trap might help to stop inflammation from causing further tissue dysfunction.

Protein-centered radicals can result from one-electron oxidation reactions of proteins most likely by mechanisms involving redox-active metals, peroxynitrite, and peroxidases [16,22,44]. Once formed, and if not trapped by DMPO, protein-centered radicals can decay by poorly understood mechanisms to form toxic end-oxidation products. One of these mechanisms is their reaction with dioxygen to form peroxyl radicals [22]. Peroxyl radicals further decompose to yield mainly aldehydes and carbonyls [22,45]. Our data show that DMPO reduces accumulation of carbonyls and cytotoxicity in macrophages primed with LPS (Figs. 1, 2, and 3). Our data also support the concept that redox active metal-catalyzed processes occurring in close proximity to the protein play a role in causing free-radical-operated protein oxidation, carbonyl accumulation, and cytotoxicity in cells stressed with LPS. In Fig. 2E we used dimethyl sulfoxide (DMSO) as a scavenger of free hydroxyl radicals and as a vehicle for DP and DPI. DMSO had no effect on LPS-induced changes in viability, nitrone adduct formation, or carbonyl content, suggesting that free hydroxyl radicals do not participate in these processes. However, because DP prevented these effects, we rationalize that DMSO might not be able to scavenge “crypto” hydroxyl radicals [19] formed by iron-cycling in close proximity to the protein. Moreover, our data suggest that DMPO can in prevent LPS-induced protein carbonylation by trapping $^{\bullet}O_2^-$, $^{\bullet}NO$ and lipid- or protein-centered radicals. However, DMPO reacts very slowly with $^{\bullet}O_2^-$ (~10 M^{-1} s^{-1}) [46] and is not known to trap $^{\bullet}NO$ [47]. Taken together, our data clearly suggest that protein-centered radicals are formed and trapped by DMPO, thereby, preventing carbonyls and cytotoxicity in cells treated with LPS.

In the absence of spin traps, protein-centered radicals decay to form oxidized and aggregated proteins [18,20]. Oxidized proteins are a source of stress for the cell, and they must be degraded through mechanisms including ubiquitination and proteasomal pathways to ensure cell survival [48]. However, we still do not know the fate of these DMPO-nitrone adducts is once they are formed inside the cell. Because trapping of macromolecule-centered radicals with DMPO inhibits cell death induced by LPS and forms nitrone adducts, it can be inferred that macromolecule-DMPO nitrone adducts are less toxic for the cell than the end-oxidation products formed when no DMPO is present (Fig. 2B). Previously, it has been shown that DMPO improves mitochondrial function in ischemic and reperfused hearts [49] and in spinal cords of a transgenic-mouse model of amyotrophic lateral sclerosis [50]. These previous observations and our data (Fig. 3E) suggest that proteins located at the mitochondrial compartment are important targets of LPS-induced, free-radical mediated, proteotoxic stress in cells, which can be prevented by trapping transient macromolecule-centered radicals with DMPO. LPS-induced cell damage increases turnover and synthesis of proteins, which might cause accumulation of oxidized and misfolded proteins in the microsomal fraction of the macrophage resulting in apoptosis [44,51]. LPS is known to induce protein oxidation [52] and endoplasmic reticulum-stress [51] in macrophages. Scavengers of ROS, such as L-ascorbate and reduced glutathione, have been shown to ameliorate endoplasmic reticulum stress induced by intracellular stress and to improve protein secretion [53]. Thus, an increase in DMPO nitrone adducts in the perinuclear region of LPS-activated macrophages (Fig. 3C and D) might indicate either accumulation of DMPO-tagged proteins guided to the microsomal fraction for processing or protein-centered radicals formed and trapped *in situ* by DMPO.

In concert with our study, a recent report by Radi's group [16] has shown peroxynitrite-mediated oxidative killing of *Trypanosome cruzi* trypomastigotes with formation of DMPO–nitrone adducts inside of phagolysosomes of J774.1 macrophages activated with interferon-γ and LPS. Importantly, their experiments targeted the detection of oxidants and protein oxidation inside the phagolysosome to explain the mechanism of trypomastigote killing by peroxynitrite, which involved formation of protein radicals inside the parasite [16]. To target the oxidative process in the phagosome, they preloaded the parasites with dihydrorhodamine which reacts with oxidants formed inside the phagolysosomes of LPS/INF-γ-activated macrophages to form the fluorescent rhodamine 123 [16]. They also preloaded the parasites with DMPO and then infected J774.1 macrophages activated with LPS/INF-γ; therefore, as expected, nitrone adducts were formed and found in this particular compartment. Because of DMPO's octanol:water coefficient (1:10) [54], it is expected that some DMPO would escape from the parasite toward the phagosome lumen and then the cytosol. However, it might not reach a sufficient concentration outside the phagolysosome to compete with the radical decay mechanisms in the cytosol and, therefore, we would not have expected trapping of any protein radical outside the phagosome [29]. It is noteworthy that what happens inside the phagosome containing parasites is just "the tip of the iceberg" compared with what happens in the whole cell in macrophages activated with LPS or LPS/INF-γ. Our cell fractionation data clearly show that DMPO nitrone adducts are formed, mainly in the mitochondrial and microsomal fractions. The latter includes the endoplasmic reticulum located in the perinuclear region of the cell which, in agreement with our confocal data (Fig. 3C and D), contains most of the nitrone adducts. In spite of a number of differences between our and Radi's experimental designs [16], our data complement Radi's and show for the first time that low doses of LPS trigger oxidation of a number of proteins inside specific subcellular locations without targeting a particular cell compartment.

Finally, we have corroborated GAPDH as one of the targets of free-radical-mediated oxidation in macrophages stressed with LPS. Oxidation of GAPDH by nonfree radical-operated mechanisms has recently been reported to lead to cell death in this model [55], and it is suggested to be a useful model for understanding some neurodegenerative disorders [32]. Our data are consistent with the formation of a GAPDH-centered radical during LPS-induced cytotoxicity in macrophages. Trapping of GAPDH-centered radicals, thus preventing GAPDH oxidation, may partially explain the protective effect of DMPO against toxicity of LPS in macrophages. The mechanism and biological significance of free-radical-operated oxidation and aggregation of GAPDH in macrophages primed with LPS is a topic under study in our laboratory.

In summary, we have demonstrated for the first time that DMPO prevented LPS-induced accumulation of protein end-oxidation products and cytotoxicity in RAW 264.7 macrophages by trapping transient protein-centered radicals. The information presented suggests a role for free-radical-operated protein oxidation in activated macrophages. Trapping specific proteins undergoing free-radical-operated oxidation inside stressed cells with DMPO blocks proteotoxic stress and "tags" specific targets that participate in cytotoxicity in stressed cells. These results warrant further corroboration and study of specific proteins labeled with DMPO during macrophage activation (e.g., carbonic

dehydrase, enolase I, prolyl hydroxylase, and heat-shock protein 80 kDa) and their role in the fate of macrophages at sites of inflammation.

Supplementary Material

Refer to Web version on PubMed Central for supplementary material.

Acknowledgments

This work was supported by the National Institute of Environmental Health Sciences (5R00ES015415-03 to DCR). KTB participation in this project was supported by the Division of Intramural Research of the NIEHS/NIH ES050171. The content is solely the responsibility of the authors and does not necessarily represent the official views of the National Institute of Environmental Health Sciences or the National Institutes of Health. The authors thank Dr. Ann Motten and Mary Mason for helping in the editing of this manuscript. The authors declare that there are no conflicts of interest.

Appendix A. supplementary material

Supplementary data associated with this article can be found in the online version at http://dx.doi.org/10.1016/j.freeradbiomed.2012.04.023.

Abbreviations

carboxy-H_2DCFDA	5-(and-6)-carboxy-2′,7′-dichlorodihydrofluorescein diacetate
DAPI	4′-6-diamidino-2-phenylindole
DMPO	5,5-dimethyl-1-pyrroline *N*-oxide
DMSO	dimethyl sulfoxide
DP	2,2′-dipyridyl
DPI	diphenyleneiodonium
ELISA	enzyme-linked immunosorbent analysis
ESR	electron-spin resonance
GAPDH	glyceraldehyde-3-phosphate dehydrogenase
H_2O_2	hydrogen peroxide
HRP	horseradish peroxidase
LC-MS/MS	liquid chromatography tandem mass spectrometry
LDH	lactate dehydrogenase
LPS	lipopolysaccharide
MTT	3-(4,5-dimethylthiazol-2-yl)-2,5-diphenyltetrazolium bromide
NAC	*N*-acetylcysteine
$^{\bullet}$NO	nitric oxide
NOX-1/2	NADPH oxidase-1 and -2

$\bullet O_2^-$	superoxide radical anion
PBN	alpha-phenyl-*N*-*tert*-butyl nitrone
PBS	phosphate-buffered saline
ROS	reactive oxygen species

References

1. Hegyi L, Hardwick SJ, Siow RC, Skepper JN. Macrophage death and the role of apoptosis in human atherosclerosis. J Hematother Stem Cell Res. 2001; 10:27–42. [PubMed: 11276357]
2. Olefsky JM, Glass CK. Macrophages, inflammation, and insulin resistance. Annu Rev Physiol. 2010; 72:219–246. [PubMed: 20148674]
3. Chawla A, Nguyen KD, Goh YP. Macrophage-mediated inflammation in metabolic disease. Nat Rev Immunol. 2011; 11:738–749. [PubMed: 21984069]
4. Murdoch C, Lewis CE. Macrophage migration and gene expression in response to tumor hypoxia. Int J Cancer. 2005; 117:701–708. [PubMed: 16106399]
5. Dalle-Donne I, Aldini G, Carini M, Colombo R, Rossi R, Milzani A. Protein carbonylation, cellular dysfunction, and disease progression. J Cell Mol Med. 2006; 10:389–406. [PubMed: 16796807]
6. Li YH, Yan ZQ, Brauner A, Tullus K. Activation of macrophage nuclear factor-kappa B and induction of inducible nitric oxide synthase by LPS. Respir Res. 2002; 3:23. [PubMed: 12323081]
7. Song JD, Lee SK, Kim KM, Kim JW, Kim JM, Yoo YH, Park YC. Redox factor-1 mediates NF-kB nuclear translocation for LPS-induced iNOS expression in murine macrophage cell line RAW 264.7. Immunology. 2007; 124:58–67. [PubMed: 18028373]
8. Lambeth JD. NOX enzymes and the biology of reactive oxygen. Nat Rev Immunol. 2004; 4:181–189. [PubMed: 15039755]
9. Clement H-W, Vazquez JF, Sommer O, Heiser P, Morawietz H, Hopt U, Schulz E, von Dobschutz E. Lipopolysaccharide-induced radical formation in the striatum is abolished in Nox2 gp91phox-deficient mice. J Neural Transm. 2010; 117:13–22. [PubMed: 19866338]
10. Cadenas E, Davies KJ. Mitochondrial free radical generation, oxidative stress, and aging. Free Radic Biol Med. 2000; 29:222–230. [PubMed: 11035250]
11. Xia Y, Zweier JL. Superoxide and peroxynitrite generation from inducible nitric oxide synthase in macrophages. Proc Natl Acad Sci USA. 1997; 94:6954–6958. [PubMed: 9192673]
12. Alhusaini S, McGee K, Schisano B, Harte A, McTernan P, Kumar S, Tripathi G. Lipopolysaccharide, high glucose and saturated fatty acids induce endoplasmic reticulum stress in cultured primary human adipocytes: salicylate alleviates this stress. Biochem Biophys Res Commun. 2010; 397:472–478. [PubMed: 20515657]
13. Gorlach A, Klappa P, Kietzmann T. The endoplasmic reticulum: folding, calcium homeostasis, signaling, and redox control. Antioxid Redox Signal. 2006; 8:1391–1418. [PubMed: 16986999]
14. Marletta MA, Yoon PS, Iyengar R, Leaf CD, Wishnok JS. Macrophage oxidation of L-arginine to nitrite and nitrate: nitric oxide is an intermediate. Biochemistry. 1988; 27:8706–8711. [PubMed: 3242600]
15. Fukuyama N, Ichimori K, Su Z, Ishida H, Nakazawa H. Peroxynitrite formation from activated human leukocytes. Biochem Biophys Res Commun. 1996; 224:414–419. [PubMed: 8702403]
16. Alvarez MN, Peluffo G, Piacenza L, Radi R. Intraphagosomal peroxynitrite as a macrophage-derived cytotoxin against internalized Trypanosoma cruzi: consequences for oxidative killing and role of microbial peroxiredoxins in infectivity. J Biol Chem. 2011; 286:6627–6640. [PubMed: 21098483]
17. Lopes de Menezes S, Augusto O. EPR detection of glutathionyl and proteintyrosyl radicals during the interaction of peroxynitrite with macrophages (J774). J Biol Chem. 2001; 276:39879–39884. [PubMed: 11518708]

18. Stadtman ER, Levine RL. Free radical-mediated oxidation of free amino acids and amino acid residues in proteins. Amino Acids. 2003; 25:207–218. [PubMed: 14661084]
19. Imlay JA, Chin SM, Linn S. Toxic D. N. A. damage by hydrogen peroxide through the Fenton reaction in vivo and in vitro. Science. 1988; 240:640–642. [PubMed: 2834821]
20. Davies MJ, Gilbert BC, Haywood RM. Radical-induced damage to proteins: e.s.r. spin-trapping studies. Free Radic Res Commun. 1991; 15:111–127. [PubMed: 1661698]
21. Ramirez DC, Gomez-Mejiba SE, Mason RP. Copper-catalyzed protein oxidation and its modulation by carbon dioxide: enhancement of protein radicals in cells. J Biol Chem. 2005; 280:27402–27411. [PubMed: 15905164]
22. Davies MJ. The oxidative environment and protein damage. Biochim Biophys Acta. 2005; 1703:93–109. [PubMed: 15680218]
23. Winterbourn CC. Reconciling the chemistry and biology of reactive oxygen species. Nat Chem Biol. 2008; 4:278–286. [PubMed: 18421291]
24. Winterbourn CC, Chan T, Buss IH, Inder TE, Mogridge N, Darlow BA. Protein carbonyls and lipid peroxidation products as oxidation markers in preterm infant plasma: associations with chronic lung disease and retinopathy and effects of selenium supplementation. Pediatr Res. 2000; 48:84–90. [PubMed: 10879804]
25. Dalle-Donne I, Rossi R, Giustarini D, Milzani A, Colombo R. Protein carbonyl groups as biomarkers of oxidative stress. Clin Chim Acta. 2003; 329:23–38. [PubMed: 12589963]
26. Davies MJ, Hawkins CL. EPR spin trapping of protein radicals. Free Radic Biol Med. 2004; 36:1072–1086. [PubMed: 15082061]
27. Janzen EG, Jandrisits LT, Shetty RV, Haire DL, Hilborn JW. Synthesis and purification of 5,5-dimethyl-1-pyrroline-*N*-oxide for biological applications. Chem Biol Interact. 1989; 70:167–172. [PubMed: 2544305]
28. Janzen EG. Spin trapping. Methods Enzymol. 1984; 105:188–198. [PubMed: 6328178]
29. Gomez-Mejiba SE, Zhai Z, Akram H, Deterding LJ, Hensley K, Smith N, Towner RA, Tomer KB, Mason RP, Ramirez DC. Immuno-spin trapping of protein and DNA radicals: ”tagging” free radicals to locate and understand the redox process. Free Radic Biol Med. 2009; 46:853–865. [PubMed: 19159679]
30. Detweiler CD, Deterding LJ, Tomer KB, Chignell CF, Germolec D, Mason RP. Immunological identification of the heart myoglobin radical formed by hydrogen peroxide. Free Radic Biol Med. 2002; 33:364–369. [PubMed: 12126758]
31. Gomez-Mejiba SE, Zhai Z, Gimenez MS, Ashby MT, Chilakapati J, Kitchin K, Mason RP, Ramirez DC. Myeloperoxidase-induced genomic DNA-centered radicals. J Biol Chem. 2010; 285:20062–20071. [PubMed: 20406811]
32. Pierce A, Mirzaei H, Muller F, De Waal E, Taylor AB, Leonard S, Van Remmen H, Regnier F, Richardson A, Chaudhuri A. GAPDH is conformationally and functionally altered in association with oxidative stress in mouse models of amyotrophic lateral sclerosis. J Mol Biol. 2008; 382:1195–1210. [PubMed: 18706911]
33. Mosmann T. J Immunol Methods. 1983; 65:55–63. [PubMed: 6606682]
34. Wardman P. Fluorescent and luminescent probes for measurement of oxidative and nitrosative species in cells and tissues: progress, pitfalls, and prospects. Free Radic Biol Med. 2007; 43:995–1022. [PubMed: 17761297]
35. Bronfman M, Loyola G, Koenig CS. Isolation of intact organelles by differential centrifugation of digitonin-treated hepatocytes using a table Eppendorf centrifuge. Anal Biochem. 1998; 255:252–256. [PubMed: 9451511]
36. Winterbourn CC, Buss IH. Protein carbonyl measurement by enzyme-linked immunosorbent assay. Methods Enzymol. 1999; 300:106–111. [PubMed: 9919514]
37. Ramirez, DC.; Mason, RP. Immuno-spin trapping: detection of protein-centered radicals. In: Costa, LG.; Maines, MD.; Reed, DJ.; Sassa, S.; Sipes, IG., editors. Current protocols in toxicoicology. Hoboken, NJ: Wiley; 2005. 17.17.11–17.17.16
38. Ramirez DC, Gomez-Mejiba SE, Corbett JT, Deterding LJ, Tomer KB, Mason RP. Cu, Zn-superoxide dismutase-driven free radical modifications: copper- and carbonate radical anion-initiated protein radical chemistry. Biochem J. 2009; 417:341–353. [PubMed: 18764780]

39. Mason RP. Using anti-5,5-dimethyl-1-pyrroline N-oxide (anti-DMPO) to detect protein radicals in time and space with immuno-spin trapping. Free Radic Biol Med. 2004; 36:1214–1223. [PubMed: 15110386]
40. Halliwell B. Antioxidant characterization. Methodology and mechanism. Biochem Pharmacol. 1995; 49:1341–1348. [PubMed: 7763275]
41. Domazou AS, Koppenol WH, Gebicki JM. Efficient repair of protein radicals by ascorbate. Free Radic Biol Med. 2009; 46:1049–1057. [PubMed: 19185609]
42. Floyd RA, Kopke RD, Choi CH, Foster SB, Doblas S, Towner RA. Nitrones as therapeutics. Free Radic Biol Med. 2008; 45:1361–1374. [PubMed: 18793715]
43. Zhai Z, Gomez-Mejiba SE, Zhu H, Lupu F, Ramirez DC. The spin trap 5,5-dimethyl-1-pyrroline *N*-oxide inhibits lipopolysaccharide-induced inflammatory response in RAW 264.7 cells. Life Sci. 2012; 90:432–439. [PubMed: 22285597]
44. van der Vlies D, Woudenberg J, Post JA. Protein oxidation in aging: endoplasmic reticulum as a target. Amino Acids. 2003; 25:397–407. [PubMed: 14661099]
45. Hawkins CL, Pattison DI, Davies MJ. Hypochlorite-induced oxidation of amino acids, peptides and proteins. Amino Acids. 2003; 25:259–274. [PubMed: 14661089]
46. Finkelstein E, Rosen GM, Rauckman EJ, Paxton J. Spin trapping of superoxide. Mol Pharmacol. 1979; 16:676–685. [PubMed: 229403]
47. Pou S, Keaton L, Surichamorn W, Frigillana P, Rosen GM. Can nitric oxide be spin trapped by nitrone and nitroso compounds? Biochim Biophys Acta. 1994; 1201:118–124. [PubMed: 7522570]
48. Jung T, Bader N, Grune T. Oxidized proteins: intracellular distribution and recognition by the proteasome. Arch Biochem Biophys. 2007; 462:231–237. [PubMed: 17362872]
49. Zuo L, Chen YR, Reyes LA, Lee HL, Chen CL, Villamena FA, Zweier JL. The radical trap 5,5-dimethyl-1-pyrroline *N*-oxide exerts dose-dependent protection against myocardial ischemia-reperfusion injury through preservation of mitochondrial electron transport. J Pharmacol Exp Ther. 2009
50. Cassina P, Cassina A, Pehar M, Castellanos R, Gandelman M, de Leon A, Robinson KM, Mason RP, Beckman JS, Barbeito L, Radi R. Mitochondrial dysfunction in SOD1G93A-bearing astrocytes promotes motor neuron degeneration: prevention by mitochondrial-targeted antioxidants. J Neurosci. 2008; 28:4115–4122. [PubMed: 18417691]
51. Gotoh T, Oyadomari S, Mori K, Mori M. Nitric oxide-induced apoptosis in RAW 264.7 macrophages is mediated by endoplasmic reticulum stress pathway involving ATF6 and CHOP. J Biol Chem. 2002; 277:12343–12350. [PubMed: 11805088]
52. Fu Y, McCormick CC, Roneker C, Lei XG. Lipopolysaccharide and interferon-gamma-induced nitric oxide production and protein oxidation in mouse peritoneal macrophages are affected by glutathione peroxidase-1 gene knockout. Free Radic Biol Med. 2001; 31:450–459. [PubMed: 11498278]
53. Malhotra JD, Miao H, Zhang K, Wolfson A, Pennathur S, Pipe SW, Kaufman RJ. Antioxidants reduce endoplasmic reticulum stress and improve protein secretion. Proc Natl Acad Sci USA. 2008; 105:18525–18530. [PubMed: 19011102]
54. Janzen EG, West MS, Kotake Y, DuBose CM. Biological spin trapping methodology. III. Octanol-water partition coefficients of spin-trapping compounds. J Biochem Biophys Methods. 1996; 32:183–190. [PubMed: 8844325]
55. Hara MR, Agrawal N, Kim SF, Cascio MB, Fujimuro M, Ozeki Y, Takahashi M, Cheah JH, Tankou SK, Hester LD, Ferris CD, Hayward SD, Snyder SH, Sawa A. S-nitrosylated, G. A. P. D. H. initiates apoptotic cell death by nuclear translocation following Siah1 binding. Nat Cell Biol. 2005; 7:665–674. [PubMed: 15951807]

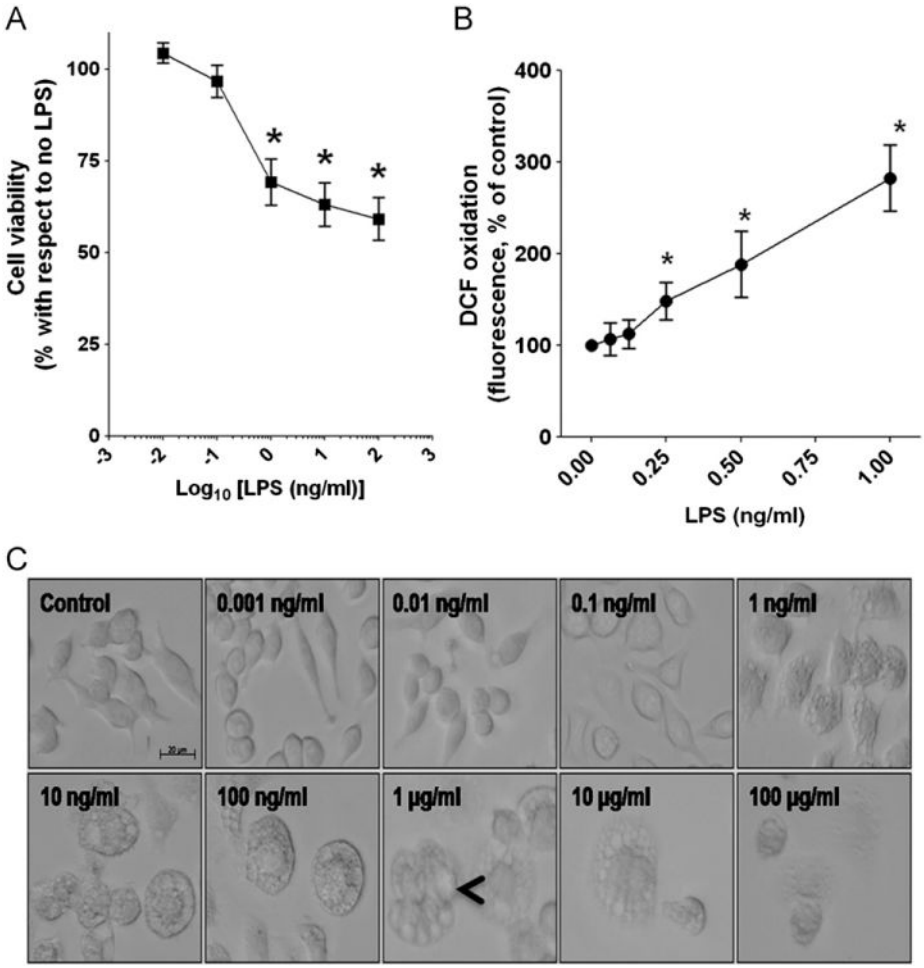

Fig. 1.

Cell viability, DCF oxidation, and morphological changes in RAW 264.7 cells primed with LPS. (A) RAW 264.7 cells were incubated for 24 h in the presence of the indicated concentrations of LPS. The concentrations of LPS are indicated in a logarithmic scale. Cell viability was assessed by the MTT reduction assay. Asterisks indicate significantly different mean values with respect to no LPS. (B) LPS-triggered increased carboxy-H_2DCFDA fluorescence in macrophages as an indication of ROS production. (C) Phase contrast images showing LPS-induced cell morphological changes. Arrowheads indicate cytoplasm vacuoles observed in macrophages treated with LPS. Data are shown as mean values ± SEM or representative data obtained from 3 independent experiments (n = 9).

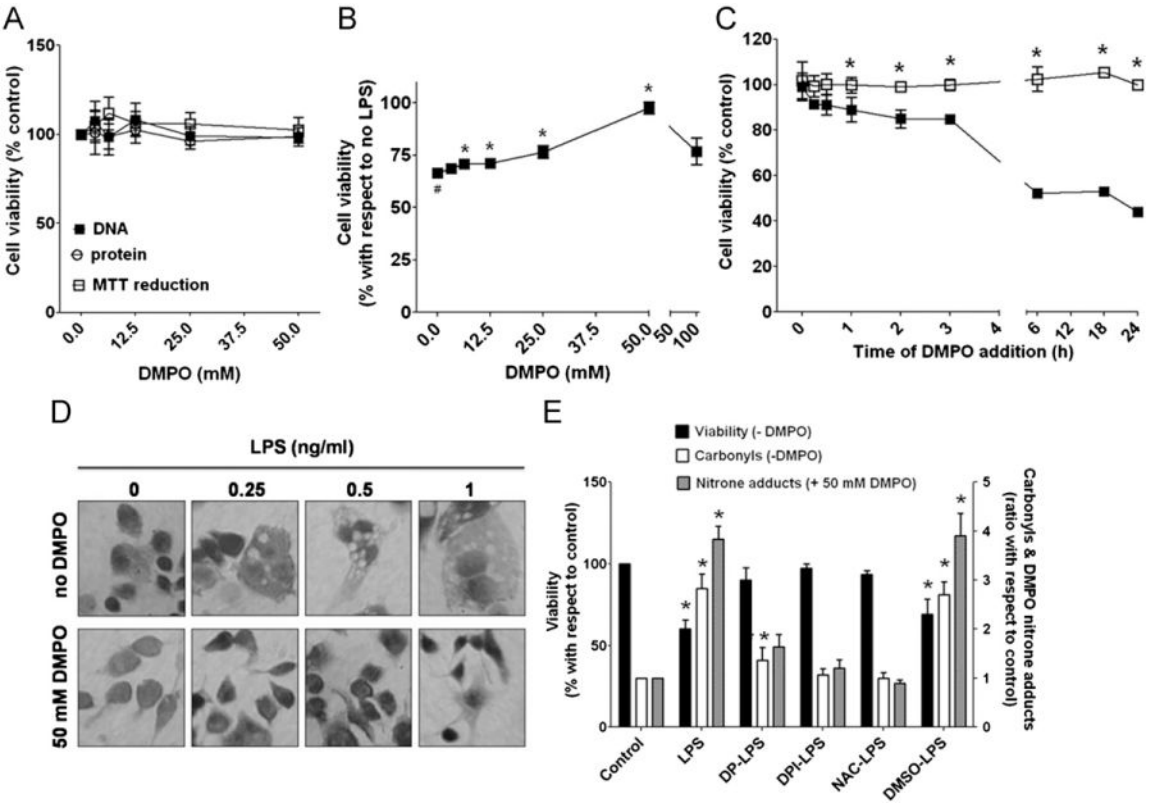

Fig. 2.

Effect of DMPO on LPS-induced oxidative damage in RAW 264.7 cells. (A) RAW 264.7 macrophages were cultured in complete medium with different concentrations of DMPO for 24 h. Cell viability was assessed by measuring cell DNA and proteins remaining bound to the plate and by the reduction of MTT to formazan. (B) RAW 264.7 cells were incubated *in vitro* for 24 h in the presence of 1 ng/ml of LPS alone (marked with #) or 1 ng/ml LPS and the indicated concentrations of DMPO, and the cell viability was assessed using the MTT assay. Asterisks show significant differences with respect to the viability of macrophages incubated with LPS alone (#). (C) Cells were incubated in the presence or absence of 1 ng/ml LPS, and DMPO was added either simultaneously with LPS (0 h) or up to 24 h after addition of LPS. Cell viability was measured 24 h after LPS addition using the MTT assay. Asterisks indicate $P < 0.05$ vs the LPS-untreated control at the same time point. (D) DMPO blocked LPS-induced morphological changes in RAW 264.7 cells as assessed by Diff-Quick staining of cells incubated for 24 h with different concentrations of LPS with or without DMPO. (E) Cells were preincubated with either 100 μM DPI, an inhibitor of NADPH oxidases, for 30 min; 100 μM DP, a chelator of ferrous iron, for 2 h; 5 mM NAC, a source of glutathione, for 4 h; or 10 mM dimethyl sulfoxide (DMSO) for 4 h. After rinsing, cells were incubated in fresh medium containing 1 ng/ml of LPS with or without 50 mM DMPO and DMSO in one experiment for 24 h. After incubation, MTT reduction was assessed as a parameter of viability. Carbonyls and DMPO–protein nitrone adducts were determined by ELISA in whole homogenates of macrophages treated with or without DMPO, respectively. Data show mean values of percentages or ratios ± SEM from three independent experiments

($n = 9$). Asterisks indicate $P < 0.05$ in comparison with cells not pretreated and incubated in complete medium with no DMPO (marked as control).

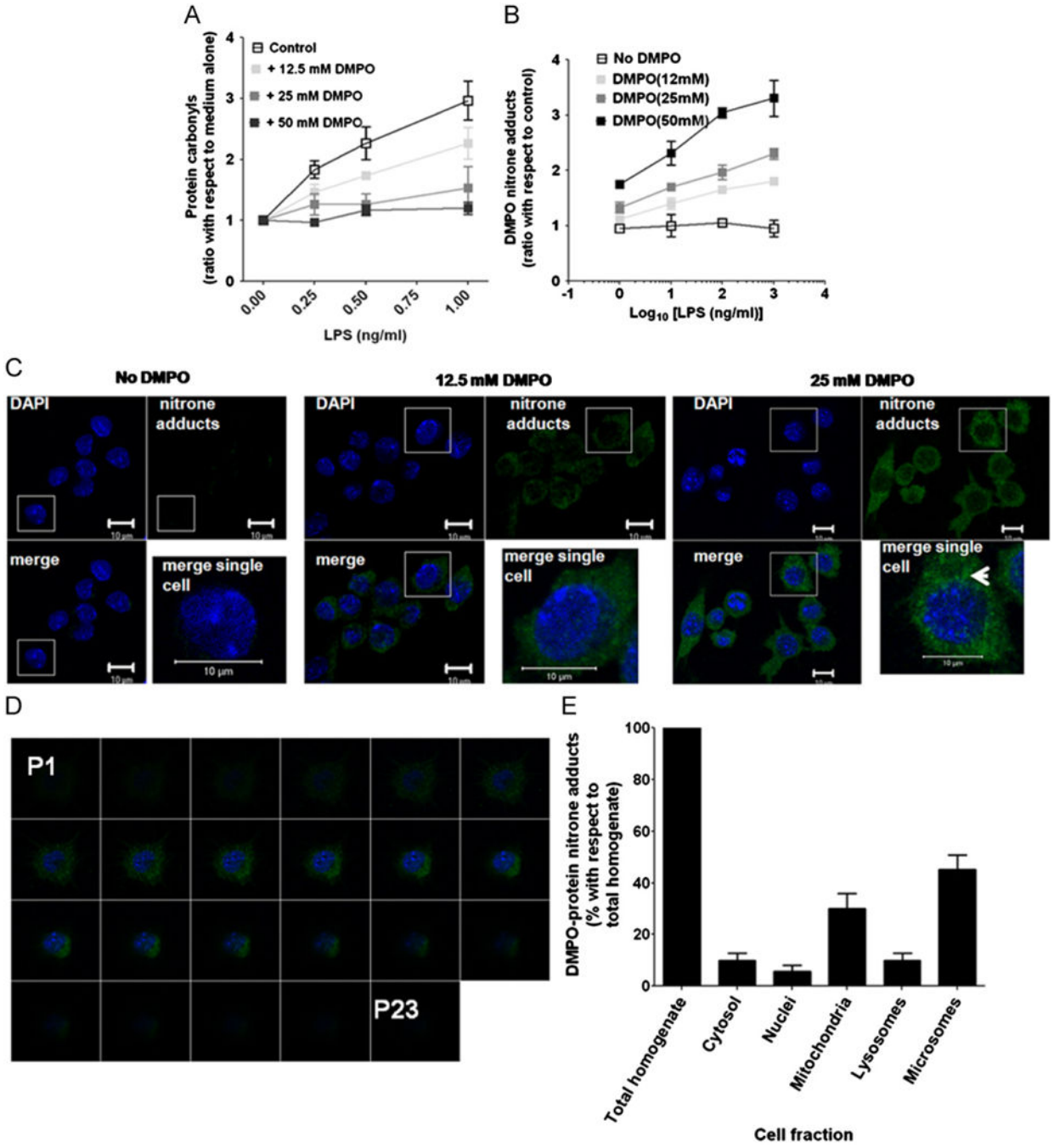

Fig. 3.

DMPO blocks carbonyl-protein adduct formation and traps protein-centered radicals in specific cell compartments. (A) ELISA of carbonyls in RAW 264.7 cells treated for 24 h with different concentrations of LPS and DMPO. (B) Cell-based ELISA of nitrone adducts in cells treated as in A. The concentrations of LPS (ng/ml) in the *x*-axes are marked as their Log_{10} value. (C) Single-plan confocal images of nitrone adducts formed in cells treated with 1 ng/ml LPS and 12.5 or 50 mM DMPO for 24 h. Green indicates nitrone adducts and blue indicates nuclei. Inset is a high-power magnification of the image of a single and

representative cell. The white arrowhead indicates the perinuclear localization of most nitrone adducts. (D) Twenty-three sequential single-plane confocal images (P1 to P23 from left to right and from top to bottom) from a representative cell treated with 1 ng/ml LPS and 50 mM DMPO for 24 h. (E) ELISA analysis of DMPO–protein nitrone adducts in different fractions of macrophages treated as in D. Data show mean values ± SEM or a representative image from three independent experiments ($n = 6$). (For interpretation of the references to color in this figure legend, the reader is referred to the web version of this article.)

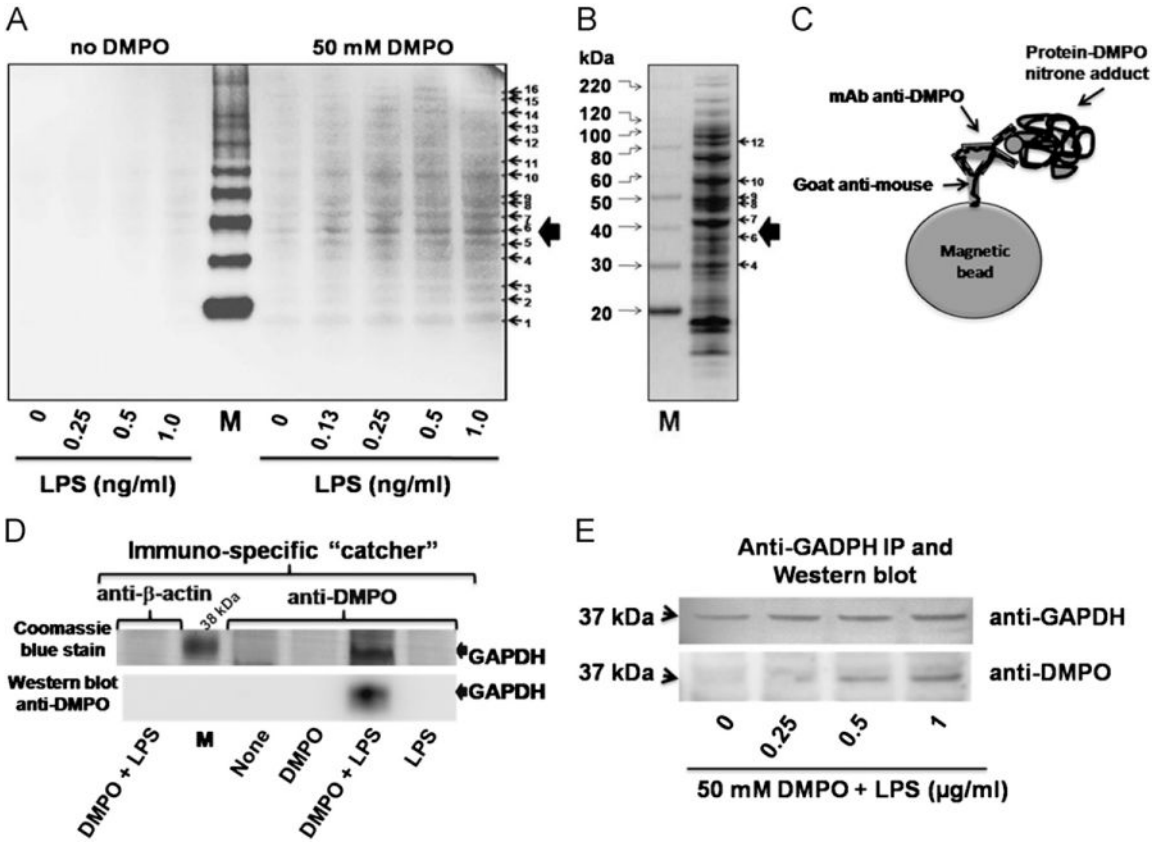

Fig. 4.

Identification of protein–DMPO nitrone adducts in homogenate of RAW 264.7 cells treated with LPS and DMPO. (A) Western blot analysis of protein–DMPO nitrone adducts in whole homogenates of cells treated with LPS and/or DMPO for 24 h. (B) Coomassie blue staining of the homogenate of cells treated with 1 ng/ml LPS and 50 mM DMPO for 24 h, separated in a reducing gel and showing 7 representative bands that correspond to anti-DMPO positive bands in A. (C) Schematic representation of an anti-DMPO molecular "catcher"—protein–DMPO nitrone adduct complex. (D) Immunoprecipitation of nitrone adducts from a homogenate of macrophages treated with or without LPS and/or DMPO with a molecular "catcher" anti-β-actin or anti-DMPO. Immunoprecipitated proteins were separated in a gel and stained with Coomassie blue for MS analysis or blotted to a nitrocellulose membrane and assayed by Western blot with the rabbit anti-DMPO antibody. (E) As D, but an anti-GAPDH molecular "catcher" was used and the membrane tested against GAPDH or nitrone adducts by Western blot. IP indicates immunoprecipitation. Data shown are a representative staining obtained from 3 independent experiments ($n = 6$). M indicates Magic Mark Western XP molecular weight marker (Invitrogen).